Dramatic Nondipole Effects in Low-Energy Photoionization: Experimental and Theoretical Study of Xe 5*s*

O. Hemmers,[1] R. Guillemin,[1,2] E. P. Kanter,[3] B. Krässig,[3] D. W. Lindle,[1] S. H. Southworth,[3] R. Wehlitz,[4] J. Baker,[1] A. Hudson,[1] M. Lotrakul,[1] D. Rolles,[5] W. C. Stolte,[1,2] I. C. Tran,[1] A. Wolska,[1,2] S. W. Yu,[1,2] M. Ya. Amusia,[6,7] K. T. Cheng,[8] L. V. Chernysheva,[7] W. R. Johnson,[9] and S. T. Manson[10]

[1]*Department of Chemistry, University of Nevada, Las Vegas, Nevada 89154-4003, USA*
[2]*Advanced Light Source, Lawrence Berkeley National Laboratory, Berkeley, California 94720, USA*
[3]*Argonne National Laboratory, Argonne, Illinois 60439, USA*
[4]*Synchrotron Radiation Center, University of Wisconsin, Stoughton, Wisconsin 53589, USA*
[5]*Fritz-Haber-Institut der Max-Planck Gesellschaft, Berlin, Germany*
[6]*The Racah Institute of Physics, The Hebrew University of Jerusalem, 91904 Jerusalem, Israel*
[7]*Ioffe Physical-Technical Institute, 194021 St. Petersburg, Russia*
[8]*Lawrence Livermore National Laboratory, University of California, Livermore, California 94550, USA*
[9]*Department of Physics, University of Notre Dame, Notre Dame, Indiana 46556, USA*
[10]*Department of Physics and Astronomy, Georgia State University, Atlanta, Georgia 30303-3083, USA*

(Received 20 January 2003; published 1 August 2003)

The Xe 5*s* nondipole photoelectron parameter γ is obtained experimentally and theoretically from threshold to ~200 eV photon energy. Significant nondipole effects are seen even in the threshold region of this valence shell photoionization. In addition, contrary to previous understanding, clear evidence of interchannel coupling among quadrupole photoionization channels is found.

DOI: 10.1103/PhysRevLett.91.053002 PACS numbers: 31.25.Eb, 32.80.Fb

Until recently, conventional wisdom had assumed nondipole effects in photoionization were negligible at relatively low photon energies, perhaps for energies up to a few keV, but certainly for photon energies below a few hundred eV [1–3]. Indeed, despite indications to the contrary [4–7], the usual practice in the field of photoionization, particularly for experiment, had been to ignore effects beyond the dipole approximation for photon energies as high as several keV. While this may be a reasonable assumption for integrated cross sections, recent work has shown it is certainly wrong for differential cross sections (i.e., photoelectron angular distributions). Experiments have shown the importance of nondipole effects in the 1–3 keV photon-energy region [8,9], in the hundreds-of-eV range [10], and, in one case, at 13 eV [11]. Concurrently, theory has predicted significant nondipole contributions to electron angular distributions for atomic valence shells down to threshold at a few tens of eV photon energy [12–14].

In addition, for dipole photoionization, interchannel coupling, which is simply configuration interaction in the continuum, has been shown to be important for most subshells of most atoms at most energies [15,16]; this work was contrary to the previous conventional wisdom that the independent-particle approximation (IPA) was generally valid away from thresholds. It had been suggested, however, that such interchannel coupling was not important in quadrupole photoionization channels [17], but recent theory has suggested that interchannel coupling can indeed be significant in quadrupole photoionization channels as well [14].

To test these two ideas, significant nondipole contributions to the photoionization of a valence shell in the threshold region, and the existence of interchannel coupling effects in quadrupole photoionization channels, we have performed a benchmark experiment on the differential photoionization cross section of Xe 5*s* from 26 eV (close to threshold) to ~200 eV to obtain the nondipole contribution to the photoelectron angular distribution which arises from interference between dipole ($E1$) and quadrupole ($E2$) channels. The differential cross section is given by [6,18–20]

$$\frac{d\sigma}{d\Omega}(\theta, \phi) = \frac{\sigma}{4\pi}\{1 + \beta P_2(\cos\theta) + (\delta + \gamma\cos^2\theta)\sin\theta\cos\phi\}, \quad (1)$$

where σ is the angle-integrated cross section, β is the dipole anisotropy parameter, $P_2(\cos\theta) = (3\cos^2\theta - 1)/2$, and δ and γ are nondipole asymmetry parameters. The coordinate axes have the positive x axis along the direction of the photon propagation vector, the z axis along the photon polarization vector, and θ and ϕ are the polar and azimuthal angles of the photoelectron momentum vector. Note, however, that the nondipole parameter δ is effectively zero for an initial s subshell [17,19].

Xe 5*s* was chosen for experimental investigation for a number of reasons. First, there have been several theoretical predictions concerning nondipole photoionization channels for Xe 5*s* [13,14,17,19]. More generally, the Xe 5*s* subshell has long provided a showcase system for studies of relativistic and many-electron interactions in

dipole atomic photoionization. Nonrelativistic, independent-particle calculations such as Hartree-Fock (HF) [21] obtain a zero in the Xe 5s partial cross section just around threshold (23.397 eV) due to the $5s \rightarrow \epsilon p$ dipole amplitude passing through a "Cooper minimum" [22]. Interchannel coupling with excitations of the 5p and 4d subshells modify the 5s partial cross section in the Cooper minimum region and produce a maximum and second minimum at higher energies [23]. Relativistic interaction in 5s photoionization is evidenced by the photoelectron anisotropy parameter $\beta < 2$ [24]. The precise positions, shapes, and magnitudes of energy-dependent features in the 5s partial cross section, β, and spin-polarization parameters are sensitive to the accuracy of theoretical treatments of relativistic and many-electron interactions [23–30]. Notably, quantitative calculation of the partial cross section and β in the Cooper minimum region requires treatment of final ionic-state electron correlation as well as interchannel coupling including coupling with satellite channels [29,30]. Finally, for s subshells, no $\ell \rightarrow \ell - 1$ dipole or $\ell \rightarrow \ell, \ell - 2$ quadrupole transitions are possible, simplifying the dependence of the dynamic properties on matrix elements and their phases and, thereby, interpretation of the results.

Measurements were made over the 26–140 eV photon-energy range at Wisconsin's Synchrotron Radiation Center (SRC) with an instrument described in [31]. Measurements over the 80–197.5 eV photon-energy range were made at the Advanced Light Source (ALS) of the Lawrence Berkeley National Laboratory with an instrument described in [32]. In both experiments, electron analyzers were positioned at sets of angles that are sensitive to different combinations of β, δ, and γ, and differences in the photoelectron intensities yielded values of $\gamma + 3\delta$. Since δ is "negligibly small" for Xe 5s in this energy range [17], the experiments essentially measured γ, which is the parameter calculated in [13,14].

To check for systematic errors in the SRC experiment, the asymmetries of several Xe $N_{4,5} - OO$ Auger-electron lines in the 3–33 eV kinetic energy range were measured. An average asymmetry of $\gamma + 3\delta = 0.004(34)$ was measured for the Auger electrons, which is consistent with zero first-order nondipole asymmetries in the limit of a two-step model [33]. In the Cooper minimum region where the 5s photopeak is relatively weak, photon energies were chosen to avoid overlapping with $N_{4,5} - OO$ Auger electrons produced by higher-order photons. Scattering of the $5p_{3/2}$ and $5p_{1/2}$ photoelectrons from the Xe background gas produced small energy-loss peaks near the 5s photopeak. The electron analyzers were operated at sufficient resolution to isolate the 5s photopeak, and a peak-fitting routine was used to determine its area.

The experiments performed at the ALS on undulator beam line 8.0 used a gas-phase time-of-flight (TOF) electron-spectroscopy system. A key characteristic for the present measurements is that the TOF method can measure photoelectron peaks at many kinetic energies and at multiple emission angles simultaneously, permitting sensitive determinations of electron angular distributions with minimal experimental uncertainty. Retarding voltages between -50 V ($h\nu = 80$ eV) and -167.5 V ($h\nu = 197.5$ eV) were applied to slow the electrons and to separate the Xe 5s from the nearby satellite lines. The neon 2p photoline was used to calibrate the analyzers because the dipole and nondipole contributions to the angular distributions are well known. Neon 2s spectra were used to determine the degree of linear polarization of the synchrotron light to be $> 99.9\%$.

Results of the measurements are shown in Fig. 1 where γ is seen to take on substantial values and vary rapidly over a fairly broad energy range in both the threshold region and the 150 eV region. Near threshold, values of γ between about ± 0.35 are found, along with a rapid

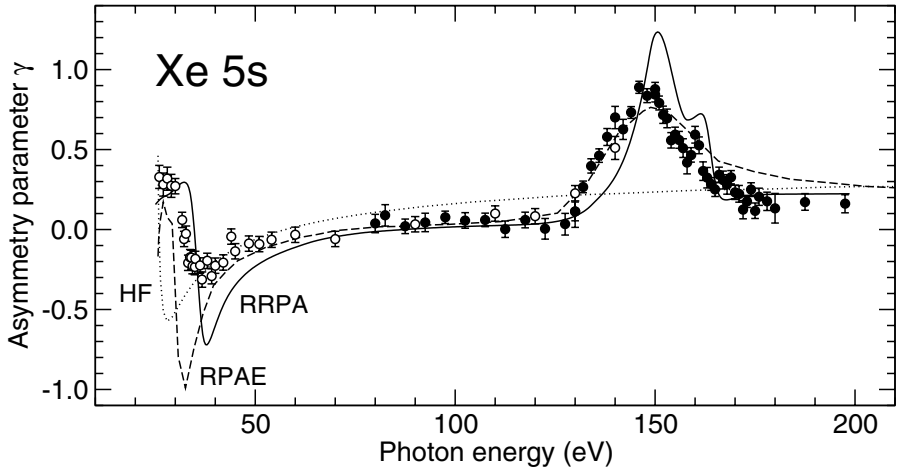

FIG. 1. Xe 5s nondipole asymmetry parameters γ measured at SRC (open circles) and ALS (closed circles) compared with our HF, random phase approximation with exchange (RPAE), and relativistic random phase approximation (RRPA) calculations.

excursion of roughly 0.65 over a small energy region. This is by far the largest nondipole effect ever measured below 100 eV. In addition, in the 150 eV region, the experimental γ is seen to reach a value of about 0.9, which translates to a major effect upon the photoelectron angular distribution.

It is important to note how these values of γ translate to the shape of the angular distribution. An excellent method of portraying the influence of nondipole photoionization is to scrutinize the forward-backward asymmetry with respect to the photon propagation direction; within the dipole approximation there is no asymmetry. From the present data the total photoelectron flux in the forward half-space exceeds the backward by a maximum of about 9% in the threshold region, and by about 25% in the 150 eV photon-energy region. At the angles actually used in the two experiments, a 14% asymmetry was measured at low energy, and a 65% asymmetry was found at higher energy. This clearly demonstrates the significance of the nondipole contributions.

It is noteworthy that in the 80–140 eV photon-energy range, where the SRC and the ALS experimental results overlap, excellent agreement between them is found. Also shown in Fig. 1 are the results of a RRPA calculation which included coupling among *all* of the single excitation channels from $5p$, $5s$, $4d$, $4p$, and $4s$ subshells, a total of 21 coupled relativistic dipole channels, and 25 coupled quadrupole channels. These calculations are similar to those of Ref. [14], except here *experimental* thresholds are used for greater accuracy. From the comparison, the theoretical RRPA result is seen to be qualitatively correct, but quantitatively somewhat off in the neighborhood of the large structures in γ, particularly in the near-threshold region where it is known from studies of the dipole asymmetry parameter β that quantitative accuracy requires inclusion of $5p$ and $4d$ satellite channels [29,30]. Note that the accuracy of the RRPA results should be essentially the same for dipole and quadrupole amplitudes.

Also shown in Fig. 1 are the results of a HF calculation and an RPAE calculation (essentially a nonrelativistic RRPA), similar to those of [13] but calculated with greater accuracy; the RPAE result also shows good qualitative agreement with experiment. All three calculations predict a similar structure in the threshold region, although RRPA is seen to be the more accurate, suggesting the importance of relativistic effects even at such low energy. The structure itself is the result of a Cooper minimum in the dipole channels. Nonrelativistically, γ is given by [6,19,23]

$$\gamma = 3\alpha\omega\frac{Q_2}{D_1}\cos(\delta_2 - \delta_1), \qquad (2)$$

where α is the fine structure constant, ω is the photon energy, Q_2 and D_1 are the $E2$ and $E1$ radial matrix elements, and δ_2 and δ_1 are the asymptotic phase shifts of the ϵd and ϵp continuum functions, respectively. Clearly, γ gets large when the dipole amplitude is small, which is exactly what happens at a Cooper minimum. Details of the energy variations of γ result from variations of the $E1$ and $E2$ amplitudes and phase shifts, and since all three calculations yield the same qualitative shape, it is essentially an IPA effect, modified significantly, however, by interchannel coupling.

Near the higher-energy structure in γ, the various theoretical results are rather different. The HF result gives no hint of structure and RPAE, which does not include coupling with $4p$ or $4s$ channels, produces structure in good agreement with the leading edge and height of the structure, but is slightly too broad and lacks the secondary structure seen in experiment at about 160 eV. The RRPA result shows reasonable overall agreement with experiment, somewhat better in the near-threshold region, but suggesting the inclusion of dipole satellite channels is still necessary, as found in studies of β in this energy region [34]. A notable feature of the RRPA is the small structure near 160 eV, which is a signature of interchannel coupling among the quadrupole channels [14]. This structure arises from the coupling of $5s \rightarrow \epsilon d$ quadrupole photoionization channels with the $4p \rightarrow \epsilon f$ shape resonances and is the first direct observation of interchannel coupling in quadrupole channels. It is emphasized that this is not an experimental artifact, but an entirely reproducible structure. But this small structure is not the only effect of interchannel coupling. The overall behavior of γ in the 130–180 eV region is affected as well as seen by the RPAE result in which coupling with $4p$ channels is omitted. Thus it is clear that electron-electron correlation in the form of interchannel coupling is necessary for an accurate description of quadrupole photoionization, just as it is for dipole channels.

In summary, measurements of the structures in the Xe $5s$ nondipole parameter γ have been made over a broad energy range. Significant nondipole effects are found even at threshold, and even larger effects in the 150 eV photon-energy region, results which certainly contradict the notion that nondipole effects occur only at high energy. Calculations show excellent qualitative agreement, and through the combination of theory and experiment, the effects of interchannel coupling in quadrupole channels were detailed, again in contrast to the conventional wisdom which suggested that IPA should be valid in the quadrupole channels. Of additional importance is that the strong, correlation-induced nondipole effects in low-energy photoionization observed here are not unique to Xe $5s$; it is expected such effects will show up in many atoms throughout the periodic table. These considerations should apply to molecules, surfaces, clusters, and solids as well. Atoms serve as a ''laboratory'' to isolate and understand these effects in *relatively* simple systems. We emphasize further refinements in theory are required to achieve quantitative agreement with experiment. Finally,

note that a very recent measurement of the Xe 5*s* nondipole parameter in the 150 eV region [35] shows qualitatively similar effects to the present results, but there are significant quantitative differences which we do not, as yet, understand.

The ANL group was supported by the Chemical Sciences, Geosciences, and Biosciences Division of the Office of Basic Energy Sciences, Office of Science, U.S. Department of Energy, Contract No. W-31-109-Eng-38. The UNLV group acknowledges support by NSF Grant No. PHY-01-40375. The work of K. T. C. was performed under the auspices of the U.S. Department of Energy by the University of California, Lawrence Livermore National Laboratory under Contract No. W-7405-ENG-48. The research of W. R. J. was supported in part by NSF Grant No. PHY-01-39928. The work of S. T. M. was supported by NSF and NASA. We are grateful for the help of the staff of the SRC and of the ALS. The University of Wisconsin SRC is supported by NSF Grant No. DMR-0084402, and the ALS (LBNL) was supported by DOE Materials Science Division, BES, OER under Contract No. DE-AC03-76SF00098.

[1] H. A. Bethe and E. E. Salpeter, *Quantum Mechanics of One- and Two-Electron Atoms* (Springer-Verlag, Berlin, 1957), pp. 248ff.
[2] S. T. Manson and D. Dill, in *Electron Spectroscopy: Theory, Techniques and Applications*, edited by C. R. Brundle and A. D. Baker (Academic Press, New York, 1978), Vol. 2, pp. 157–195.
[3] A. F. Starace, in *Handbuch der Physik*, edited by W. Mehlhorn (Springer-Verlag, Berlin, 1982), Vol. 31, pp. 1–121.
[4] M. O. Krause, Phys. Rev. **177**, 151 (1969).
[5] J. W. Cooper and S. T. Manson, Phys. Rev. **177**, 157 (1969).
[6] M. Ya. Amusia, P. U. Arifov, A. S. Baltenkov, A. A. Grinberg, and S. G. Shapiro, Phys. Lett. **47A**, 66 (1974).
[7] A. Ron, R. H. Pratt, and H. K. Tseng, Chem. Phys. Lett. **47**, 377 (1977).
[8] B. Krässig, M. Jung, D. S. Gemmell, E. P. Kanter, T. LeBrun, S. H. Southworth, and L. Young, Phys. Rev. Lett. **75**, 4736 (1995).
[9] M. Jung, B. Krässig, D. S. Gemmell, E. P. Kanter, T. LeBrun, S. H. Southworth, and L. Young, Phys. Rev. A **54**, 2127 (1996).
[10] O. Hemmers, G. Fisher, P. Glans, D. L. Hansen, H. Wang, S. B. Whitfield, R. Wehlitz, J. C. Levin, I. A. Sellin, R. C. C. Perera, E. W. B. Dias, H. S. Chakraborty, P. C. Deshmukh, S. T. Manson, and D. W. Lindle, J. Phys. B **30**, L727 (1997).
[11] N. L. S. Martin, D. B. Thompson, R. P. Bauman, C. D. Caldwell, M. O. Krause, S. P. Frigo, and M. Wilson, Phys. Rev. Lett. **81**, 1199 (1998).
[12] V. K. Dolmatov and S. T. Manson, Phys. Rev. Lett. **83**, 939 (1999).
[13] M. Ya. Amusia, A. S. Baltenkov, L. V. Chernysheva, Z. Felfli, and A. Z. Msezane, Phys. Rev. A **63**, 052506 (2001).
[14] W. R. Johnson and K. T. Cheng, Phys. Rev. A **63**, 022504 (2001).
[15] E. W. B. Dias, H. S. Chakraborty, P. C. Deshmukh, S. T. Manson, O. Hemmers, P. Glans, D. L. Hansen, H. Wang, S. B. Whitfield, D. W. Lindle, R. Wehlitz, J. C. Levin, I. A. Sellin, and R. C. C. Perera, Phys. Rev. Lett. **78**, 4553 (1997).
[16] D. L. Hansen, O. Hemmers, H. Wang, D. W. Lindle, P. Focke, I. A. Sellin, C. Heske, H. S. Chakraborty, P. C. Deshmukh, and S. T. Manson, Phys. Rev. A **60**, R2641 (1999).
[17] A. Derevianko, W. R. Johnson, and K. T. Cheng, At. Data Nucl. Data Tables **73**, 153 (1999).
[18] A. Bechler and R. H. Pratt, Phys. Rev. A **39**, 1774 (1989); **42**, 6400 (1990).
[19] J. W. Cooper, Phys. Rev. A **42**, 6942 (1990); **45**, 3362 (1992); **47**, 1841 (1993).
[20] M. Ya. Amusia and V. K. Dolmatov, Sov. Phys. JETP **52**, 840 (1980).
[21] D. J. Kennedy and S. T. Manson, Phys. Rev. A **5**, 227 (1972).
[22] J. W. Cooper, Phys. Rev. **128**, 681 (1962).
[23] M. Ya. Amusia and N. A. Cherepkov, Case Stud. At. Phys. **5**, 47 (1975).
[24] J. L. Dehmer and D. Dill, Phys. Rev. Lett. **37**, 1049 (1976).
[25] W. R. Johnson and K. T. Cheng, Phys. Rev. Lett. **40**, 1167 (1978).
[26] N. A. Cherepkov, Phys. Lett. **66A**, 204 (1978).
[27] W. Ong and S. T. Manson, Phys. Rev. A **19**, 688 (1979).
[28] K.-N. Huang and A. F. Starace, Phys. Rev. A **21**, 697 (1980).
[29] G. Wendin and A. F. Starace, Phys. Rev. A **28**, 3143 (1983).
[30] J. Tulkki, Phys. Rev. Lett. **62**, 2817 (1989).
[31] B. Krässig, J.-C. Bilheux, R. W. Dunford, D. S. Gemmell, S. Hasegawa, E. P. Kanter, S. H. Southworth, L. Young, L. A. LaJohn, and R. H. Pratt, Phys. Rev. A **67**, 022707 (2003).
[32] O. Hemmers, S. B. Whitfield, P. Glans, H. Wang, D. W. Lindle, R. Wehlitz, and I. A. Sellin, Rev. Sci. Instrum. **69**, 3809 (1998).
[33] N. M. Kabachnik and I. P. Sazhina, J. Phys. B **29**, L515 (1996).
[34] O. Hemmers, S. T. Manson, M. M. Sant'Anna, P. Focke, H. Wang, I. A. Sellin, and D. W. Lindle, Phys. Rev. A **64**, 022507 (2001).
[35] S. Ricz, R. Sankari, Á. Kövér, M. Jurvansuu, D. Varga, J. Nikkinen, T. Ricsoka, H. Aksela, and S. Aksela, Phys. Rev. A **67**, 012712 (2003).